Pseudoscalar Transition Form Factors and the Hadronic Light-by-Light Contribution to a_μ

Antoine Gérardin
Jana Guenther
Lukas Varnhorst
Willem Verplanke
[On Behalf of the Budapest-Marseille-Wuppertal Collaboration]

September 8th, 2022 Fifth Plenary Workshop of the Muon g-2 Theory Initiative, Edinburgh

Motivation

- The error on the theory calculation of the muon $g-2$ is dominated by two hadronic contributions.

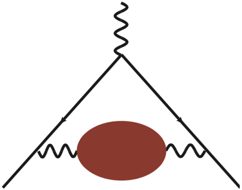

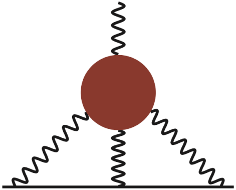

	LO HVP	**HLbL**
Contribution to $a_\mu \times 10^{11}$:	6931 ± 40	90 ± 17 [WP, 2020]

- An error of $\sim 10\%$ on the HLbL is needed for future experimental precision.
  $\rightarrow$ Difficult because it's a four-point function.
- Two independent approaches to calculate the HLbL contribution
  1. Direct lattice calculation of the four-point function.
  2. Dispersive: data-driven (cross-section, form factors..).

  $\rightarrow$ Lattice QCD can provide valuable input to dispersive approach.
  $\rightarrow$ Agreement between two approaches is an important cross-check!

Motivation

https://muon-gm2-theory.illinois.edu/white-paper/

Contributions	Value $\times 10^{11}$
π^0, η, η'-poles	93.8(4.0)
π, K-loops/boxes	-16.4(0.2)
$\pi\pi$ scattering	-8(1)
scalars + tensors	-1(3)
axial vectors	6(6)
u, d, s-loops / short distance	15(10)
c-loop	3(1)
Total	92(19)

1. π^0-pole
   - Contribution has been determined on the lattice by Mainz (Gérardin et al., 2016, 2019). Preliminary results by ETM (Burri et al., 2022).
   - Also computed in data-driven dispersive framework (Hoferichter et al., 2018).
2. η, η'-pole
   - No lattice nor dispersive results (but $\sim 1/3$ of the total pseudoscalar pole contribution)
   - Transition Form Factor not well-known in relevant kinematical region.
   - Challenges for lattice QCD: mixing between η, η' and sizable disconnected diagrams.

Motivation

- In the dispersive framework, the 'master equation' relates the Pseudoscalar Transition Form Factors (**TFF**s) to pseudoscalar (p) pole contributions to a_μ^{p-pole} (Knecht and Nyffeler, 2002)

$$a_\mu^{p-pole} = \left(\frac{\alpha_e}{\pi}\right)^3 \int_0^\infty dQ_1 \int_0^\infty dQ_2 \int_{-1}^1 d\tau \left[w_1(Q_1, Q_2, \tau)\mathscr{F}_{p\gamma^*\gamma^*}(-Q_1^2, -Q_3^2)\mathscr{F}_{p\gamma^*\gamma^*}(-Q_2^2, 0) \right.$$
$$\left. + w_2(Q_1, Q_2, \tau)\mathscr{F}_{p\gamma^*\gamma^*}(-Q_1^2, -Q_2^2)\mathscr{F}_{p\gamma^*\gamma^*}(-Q_3^2, 0)\right]$$

- $Q_3^2 = Q_1^2 + Q_2^2 + 2\tau Q_1 Q_2$
- $\tau = \cos\theta$
- θ angle between Q_1 & Q_2

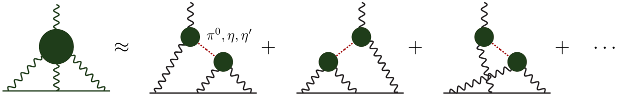

Figure 1: HLbL diagram and its leading contributions resulting from π^0, η, η' pseudoscalar exchanges.

Motivation

- In the dispersive framework, the 'master equation' relates the Pseudoscalar Transition Form Factors (**TFFs**) to pseudoscalar (p) pole contributions to a_μ^{p-pole} (Knecht and Nyffeler, 2002)

$$a_\mu^{p-pole} = \left(\frac{\alpha_e}{\pi}\right)^3 \int_0^\infty dQ_1 \int_0^\infty dQ_2 \int_{-1}^{1} d\tau \left[w_1(Q_1, Q_2, \tau) \mathscr{F}_{p\gamma^*\gamma^*}(-Q_1^2, -Q_3^2) \mathscr{F}_{p\gamma^*\gamma^*}(-Q_2^2, 0) + w_2(Q_1, Q_2, \tau) \mathscr{F}_{p\gamma^*\gamma^*}(-Q_1^2, -Q_2^2) \mathscr{F}_{p\gamma^*\gamma^*}(-Q_3^2, 0) \right]$$

We recognize two main objects

1. The TFFs $\mathscr{F}_{p\gamma^*\gamma^*}(q_1^2, q_2^2)$
2. The weight functions $w_i(q_1, q_2, \tau)$

$\mathscr{F}_{p\gamma^*\gamma^*}(q_1^2, q_2^2)$ encodes the interaction between a pseudoscalar and two virtual photons. E.g. for the pion

$\mathscr{F}_{\pi^0\gamma^*\gamma^*}(q_1^2, q_2^2) =$ 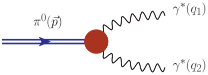

Motivation

- In the dispersive framework, the 'master equation' relates the Pseudoscalar Transition Form Factors (**TFFs**) to pseudoscalar (p) pole contributions to a_μ^{p-pole} (Knecht and Nyffeler, 2002)

$$a_\mu^{p-pole} = \left(\frac{\alpha_e}{\pi}\right)^3 \int_0^\infty dQ_1 \int_0^\infty dQ_2 \int_{-1}^{1} d\tau \left[w_1(Q_1, Q_2, \tau) \mathcal{F}_{p\gamma^*\gamma^*}(-Q_1^2, -Q_3^2) \mathcal{F}_{p\gamma^*\gamma^*}(-Q_2^2, 0) \right.$$
$$\left. + w_2(Q_1, Q_2, \tau) \mathcal{F}_{p\gamma^*\gamma^*}(-Q_1^2, -Q_2^2) \mathcal{F}_{p\gamma^*\gamma^*}(-Q_3^2, 0) \right]$$

We recognize two main objects

1. The TFFs $\mathcal{F}_{p\gamma^*\gamma^*}(q_1^2, q_2^2)$
2. The weight functions $w_i(q_1, q_2, \tau)$

Weight functions are peaked at low spacelike Q^2 so lattice QCD is the perfect method.

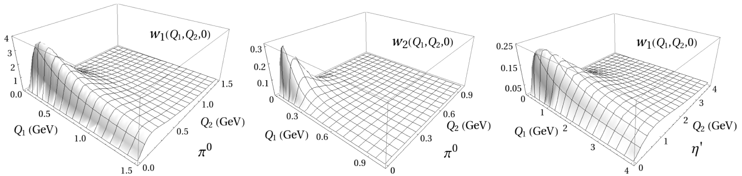

Phenomenology

- Normalization of TFF related to partial decay widths $\Gamma(p \to \gamma\gamma)$,

$$\Gamma(p \to \gamma\gamma) = \frac{\pi \alpha_e^2 m_p^3}{4} \mathscr{F}_{p\gamma^*\gamma^*}(0,0)$$

- Current values are:

  1. $\Gamma(\pi^0 \to \gamma\gamma) = 7.802(0.117)$ eV (Larin et al., 2020).
  2. $\Gamma(\eta \to \gamma\gamma) = 0.516(0.18)$ keV (PDG, 2020).
  3. $\Gamma(\eta' \to \gamma\gamma) = 4.28(0.19)$ keV (PDG, 2020).

  $\to$ Errors are relatively small (few %), so can be really useful to combine with lattice data, especially for η, η'.

- Such a constraint already tested for pion TFF in (Gérardin et al., 2019), reduced total error on $a_\mu^{\pi-\mathrm{pole}}$ by more than 30%.

Experimental Data TFF η, η'

(Aoyama et al., 2020)

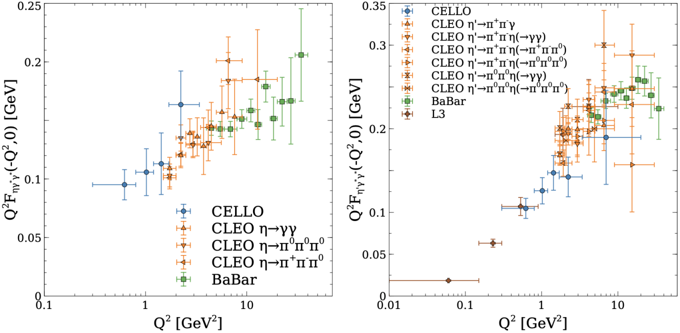

- A lot of experimental data avalaible for TFF in singly virtual (SV) regime at large Q^2.
- No data in regime where both photons are virtual below 6 GeV^2.
- Absence of precise data at low Q^2, important region for $a_\mu^{\mathrm{p-pole}}$ $\rightarrow$ can be provided by lattice QCD.
- Combination of lattice and experimental data can also be an interesting comparison to pure lattice result.

Transition Form Factor from the Lattice

The TFF for a pseudoscalar meson is defined by the matrix elements $M_{\mu\nu}$ (Ji and Jung, 2001) (Gérardin et al., 2016)

$$M_{\mu\nu}(p,q_1) = i\int d^4x\, e^{iq_1\cdot x}\langle\Omega|\, T\{J_\mu(x)J_\nu(0)\}\,|P(\vec{p})\rangle = \varepsilon_{\mu\nu\alpha\beta}\, q_1^\alpha q_2^\beta \mathscr{F}_{P\gamma^*\gamma^*}(q_1^2,q_2^2)$$

where J_μ is the EM current. (Euclidean) Matrix elements are related to 3-point correlation function $C^{(3)}_{\mu\nu}$ on lattice

$$C^{(3)}_{\mu\nu}(\tau,t_P) = a^6\sum_{\vec{x},\vec{z}}\langle J_\mu(\vec{z},\tau+t_P)J_\nu(\vec{0},t_P)P^\dagger(\vec{x},0)\rangle e^{i\vec{p}\cdot\vec{x}}e^{-i\vec{q}_1\cdot\vec{z}}$$

where τ is the time-separation between the two EM currents and

1. In the Euclidean:

$$M^E_{\mu\nu} = \frac{2E_P}{Z_P}\int_{-\infty}^{\infty} d\tau\, e^{\omega_1\tau}\tilde{A}_{\mu\nu}(\tau) \qquad \text{with } \tilde{A}_{\mu\nu} \sim C^{(3)}_{\mu\nu}$$

2. E_P, Z_P energy and overlap of the pseudoscalar that are extracted from two-point correlations functions.
3. $q_1 = (\omega_1,\vec{q}_1)$ and $q_2 = (E_P-\omega_1, \vec{p}-\vec{q}_1)$

Reach in (q_1^2, q_2^2) plane

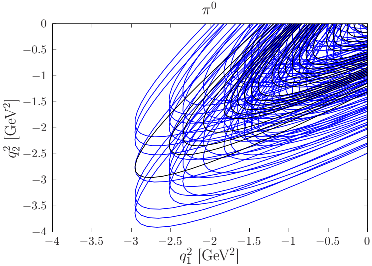

- We have a dense covering of the whole (q_1^2, q_2^2) plane.
- In the rest of the presentation we only display TFF for two regimes
  (1) $q_1^2 = q_2^2$ (doubly-virtual)
  (2) $q_1^2 = 0$, $q_2^2 \neq 0$ (singly-virtual).

Correlation Function on the Lattice: Wick Contractions

$$C^{(3)}_{\mu\nu}(\tau, t_P) = a^6 \sum_{\vec{x},\vec{z}} \langle J_\mu(\vec{z}, \tau + t_P) J_\nu(\vec{0}, t_P) P^\dagger(\vec{x}, 0)\rangle e^{i\vec{p}\cdot\vec{x}} e^{-i\vec{q}_1\cdot\vec{z}}$$

The correlation function receives contributions from (potentially) four different Wick contractions

1. - For the π^0

   $$P_{\pi^0}(x) = \frac{1}{\sqrt{2}} \left(\overline{u}\gamma_5 u(x) - \overline{d}\gamma_5 d(x)\right)$$

   ! We work in the isospin limit $\Rightarrow$ (2) and (4) do not contribute.

   ! Diagram (3) is small $\mathcal{O}(1-2\%)$ (Gérardin et al., 2019).

2. - For the η, η'

   $$P_{\eta_8}(x) = \frac{1}{\sqrt{6}} \left(\overline{u}\gamma_5 u(x) + \overline{d}\gamma_5 d(x) - 2\overline{s}\gamma_5 s(x)\right)$$

   $$P_{\eta_0}(x) = \frac{1}{\sqrt{3}} \left(\overline{u}\gamma_5 u(x) + \overline{d}\gamma_5 d(x) + \overline{s}\gamma_5 s(x)\right)$$

   ! **All** four diagrams contribute.

   ! Disconnected diagram (2) is large!

   ! η_8 and η_0 mix to create physical η, η'.

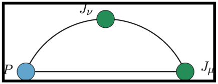

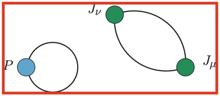

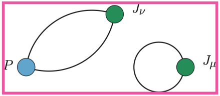

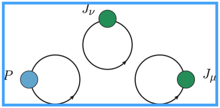

Gauge Ensembles

$2+1+1$ dynamical staggered fermions with 4 steps of stout smearing (subset of ensembles used for the LO HVP calculation (Borsanyi et al., 2021))

- Gauge ensembles at (nearly) physical pion & kaon mass.
- Exploit up to six different lattice spacings ranging between [0.0640 - 0.1315] fm.
- Consider boxes of $\sim 3, 4$ and 6 fm for finite-size effect studies.
- Ensembles in isosymmetric limit ($\rightarrow$ no mixing between π^0 and $\eta^{(\prime)}$).

Spectroscopy of the η, η' Mesons

Extraction $\eta^{(\prime)}$ masses

- From the quark model, the SU(3) octet η_8 and singlet η_0 states are

$$O_8 = \frac{1}{\sqrt{6}}\left(\bar{u}\gamma_5 u + \bar{d}\gamma_5 d - 2\bar{s}\gamma_5 s\right)$$
$$O_0 = \frac{1}{\sqrt{3}}\left(\bar{u}\gamma_5 u + \bar{d}\gamma_5 d + \bar{s}\gamma_5 s\right)$$

- Consider matrix of correlators

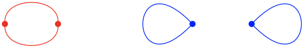

$$C(t) = \begin{pmatrix} \langle O_8(t)O_8^\dagger(0)\rangle & \langle O_8(t)O_0^\dagger(0)\rangle \\ \langle O_0(t)O_8^\dagger(0)\rangle & \langle O_0(t)O_0^\dagger(0)\rangle \end{pmatrix}$$
$$= \begin{pmatrix} \frac{1}{3}\left(C_\ell + 2C_s + 4D_{\ell s} - 2D_{\ell\ell} - 2D_{ss}\right) & \frac{\sqrt{2}}{3}\left(C_\ell + D_{\ell s} + D_{ss} - C_s - 2D_{\ell\ell}\right) \\ \frac{\sqrt{2}}{3}\left(C_\ell + D_{\ell s} + D_{ss} - C_s - 2D_{\ell\ell}\right) & \frac{1}{3}\left(2C_\ell + C_s - 4D_{\ell\ell} - 4D_{\ell s} - D_{ss}\right) \end{pmatrix}$$

- The spectral decomposition of $\langle O_8(t)O_8^\dagger(0)\rangle$ takes the form

$$\langle O_8(t)O_8^\dagger(0)\rangle = \frac{Z_8^\eta Z_8^\eta}{2E_\eta} e^{-E_\eta t} + \ldots$$

- However, a standard technique to extract ground states and excitations is a Generalized Eigenvalue Problem (GEVP)

$$C(t)v_n(t,t_0) = \lambda_n(t,t_0)C(t_0)v_n(t,t_0)$$

where the eigenvalues λ_n are related to the meson mass through

$$m_n^{\mathrm{eff}}(t) = \log\left(\frac{\lambda_n(t,t_0)}{\lambda_n(t+1,t_0)}\right), \qquad n = \eta, \eta'$$

Choice of Interpolating Operator

1. Classification of the staggered mesonic operator by Golterman (Golterman, 1986).
2. Two (taste-singlet) operators couple to the $\eta^{(\prime)}$ mesons:

- **3-link operator** $\mathcal{O}_3$ (couples to spin $\otimes$ taste $= \gamma_4\gamma_5 \otimes 1$ and $1 \otimes \gamma_4\gamma_5$), defined as (Altmeyer et al., 1993)

$$\mathcal{O}_3(x) = \frac{1}{6}\sum_{ijk} \varepsilon_{ijk}\overline{\chi}(x)[\eta_i\Delta_i[\eta_j\Delta_j[\eta_k\Delta_k]]]\chi(x) \equiv \overline{\chi}(x)\hat{O}_3\chi(x)$$

Symmetric shift $\quad \Delta_\mu\chi(x) = \frac{1}{2}\left[U_\mu(x)\chi(x+\hat{\mu}) + U_\mu^\dagger(x-\hat{\mu})\chi(x-\hat{\mu})\right]$

  - Con: Oscillating parity partner state (scalar).

- **4-link operator** $\mathcal{O}_4$ (couples to $\gamma_5 \otimes 1$), defined as

$$\xrightarrow{\text{Used in analysis}} \boxed{\mathcal{O}_4(x) = \frac{1}{2}\eta_4(x)\left[\overline{\chi}(x)\hat{O}_3\chi_+(x) + \overline{\chi}_+(x)\hat{O}_3\chi(x)\right]}$$

$$\chi_+(x) = U_0(x)\chi(x+\hat{0})$$

  - Con: Non-local in time.
  - Pro: Parity partner state contribution is highly suppressed.

Correlation Functions

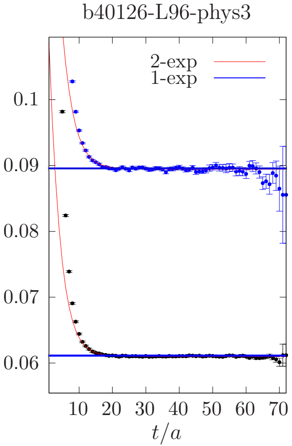

(a)

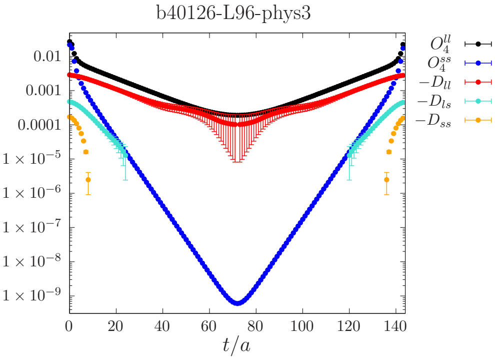

(b)

- Very precise data for the π^0 effective mass.
- We reach the gauge noise for the disconnected correlators.

Analysis Techniques (Effective Mass $\eta^{(\prime)}$)

1. 1.1 ETM observed that there are very little excited states in the disconnected diagrams (Michael et al., 2013).

   1.2 Remove excited states in *connected* correlation function $C_{\ell,s}$ by fitting it to a one-exponential fit

$$C_{\ell,s}(t) = A_{\ell,s}\left(\exp(-E_{\ell,s}t) + \exp(-E_{\ell,s}(T-t))\right),$$
$$D_{ii}(t) = \text{unchanged}, \qquad i = \ell, s,$$

   in region where excited states are highly suppressed $\longrightarrow$ Replace $C_{\ell,s}$ by fit result in the GEVP (Neff et al., 2001).

2. 2.1 For $|\vec{p}| = 0$ we observe quite large autocorrelations between timeslices (Aoki et al., 2007).

   2.2 Instead of $C(t)$ we consider $\boxed{C'(t) \equiv C(t) - C(t+\Delta t)}$ (here: $\Delta t/a = 2$) in the GEVP (Ottnad and Urbach, 2018)
   $\rightarrow$ Reduces correlations between time-slices and improves point error.
   $\rightarrow$ Removes (potential) bias in disconnected correlators due to incorrect sampling topological charge.

Effective Mass and Mixing Parameters

1. Effective mass is extracted from 1-exp fit to eigenvalues of the GEVP system.

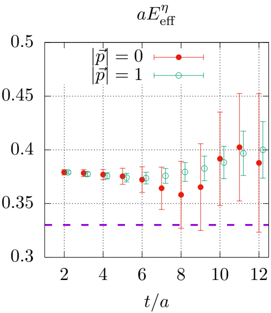

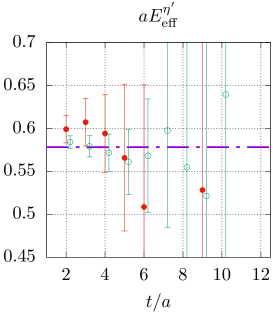

- m_η larger than physical value (purple dashed line)
- $m_{\eta'}$ around physical value.

2. Overlap factors with our interpolating operators are given by

$$A_i^{(n)} = \sqrt{2E^{(n)}} \frac{\sum_{j=1}^{N} C_{ij}(t) v_j^{(n)}(t,t_0)}{\sqrt{(v_n(t,t_0), C(t) v_n(t,t_0)) \left(\exp(-E^{(n)}t) \left(1 - e^{-E^{(n)}\Delta t}\right)\right)}}.$$

where $i = 0,8$ and $n = \eta, \eta'$.

3. Error on mass and overlap are propagated through the entire analysis of the TFF.

η, η' Transition Form Factors

Correlation Function on the Lattice: Wick Contractions

$$C^{(3)}_{\mu\nu}(\tau, t_P) = a^6 \sum_{\vec{x},\vec{z}} \langle J_\mu(\vec{z}, \tau + t_P) J_\nu(\vec{0}, t_P) P^\dagger(\vec{x}, 0)\rangle e^{i\vec{p}\cdot\vec{x}} e^{-i\vec{q}_1\cdot\vec{z}}.$$

The correlation function receives contributions from (potentially) four different Wick contractions

1. • For the π^0

   $$P_{\pi^0}(x) = \frac{1}{\sqrt{2}}\left(\overline{u}\gamma_5 u(x) - \overline{d}\gamma_5 d(x)\right).$$

   ! We work in the isospin limit $\Rightarrow$ (2) and (4) do not contribute.

   ! Diagram (3) is small $\mathcal{O}(1-2\%)$

2. • For the η, η'

   $$P_{\eta_8}(x) = \frac{1}{\sqrt{6}}\left(\overline{u}\gamma_5 u(x) + \overline{d}\gamma_5 d(x) - 2\overline{s}\gamma_5 s(x)\right),$$

   $$P_{\eta_0}(x) = \frac{1}{\sqrt{3}}\left(\overline{u}\gamma_5 u(x) + \overline{d}\gamma_5 d(x) + \overline{s}\gamma_5 s(x)\right).$$

   ! **All** four diagrams contribute.

   ! Disconnected Diagram (2) is large!

   ! η_8 and η_0 mix to create physical η, η'.

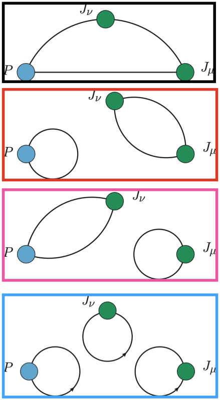

Some notation: Pseudoscalar is indicated by P and vector current by V, and a 'disconnection' by a hyphen. So (1) is PVV, (2) is P-VV (3) is PV-V and (4) P-V-V.

π^0 TFF on one ensemble

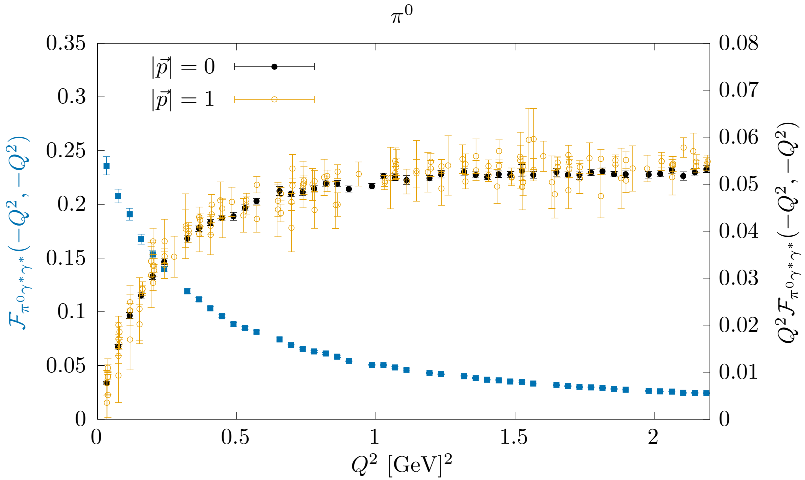

- $L/a = 96$, $a = 0.0640$ fm (6 fm box).
- Good agreement between two frames of the π^0: $\vec{p} = \vec{0}$ & $\vec{p} = \frac{2\pi}{L}(0,0,1)$.
- Error on TFF grows with decreasing Q^2.

Volume Effects π^0 TFF

- Smaller volumes reduce the cost of simulations drastically.
  $\rightarrow$ Could be useful for η, η' TFF where the noise/signal ratio increases rapidly.
- To test this possibility we study finite size effects (FSE) for the π^0 (precise data)
  $\rightarrow$ Compare signal at $a = 0.0640$ fm between 6fm and 3fm box

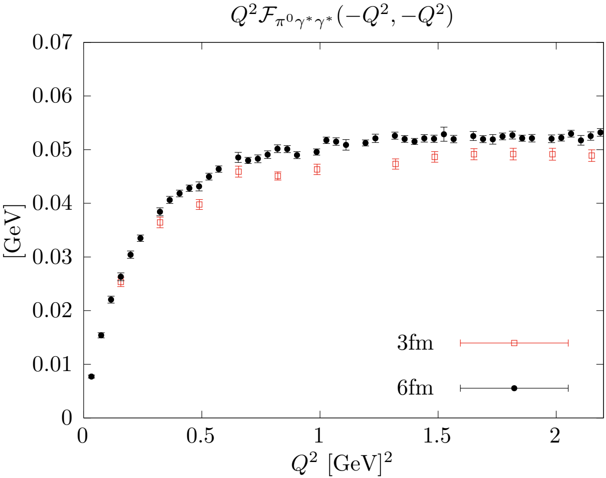

Volume Effects π^0 TFF

- We see a discrepancy between the two box sizes.
- *Backward propagating pions* may contribute signifcantly to correlation function if time-exent is relatively small (for details see (Gérardin et al., 2016)).

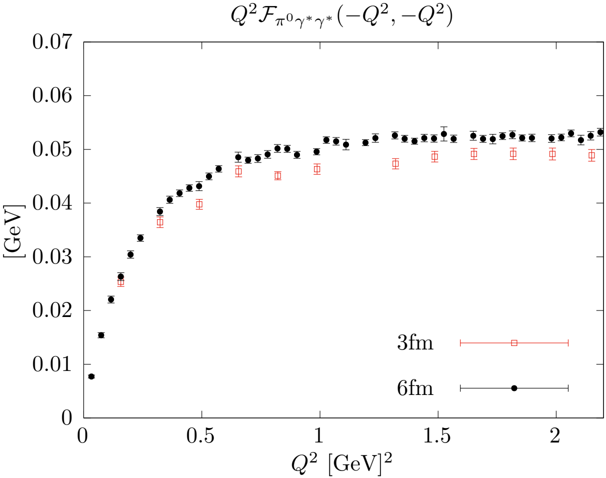

Volume Effects π^0 TFF

- We see a discrepancy between the two box sizes.
- *Backward propagating pions* may contribute signifcantly to correlation function if time-exent is relatively small (for details see (Gérardin et al., 2016)).

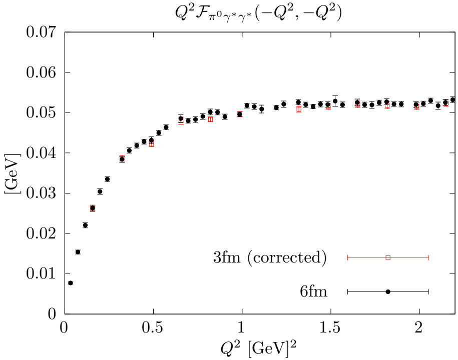

- Discrepancy can be satisfactorily explained by FTE correction
- We do not observe significant FSE for the π^0 and **thus compute the η, η' TFFs mainly on small volumes (3fm and 4fm)**.

Analysis (TFF η, η')

- Noise/signal ratio is relatively large for η, η' TFF.
- Besides addings more statistics we can consider other techniques to improve the signal/noise ratio.
- Reminder: the correlation function we consider is

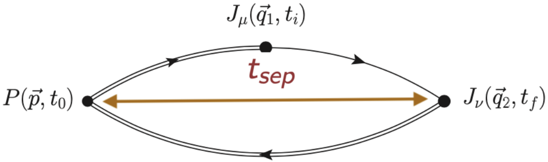

- For the π^0 one can simply use a very large t_{sep} (no noise problem).
  $\rightarrow$ May be unnecessarily large for η, η'.
- Idea: compute the correlation function for different values of t_{sep}.
  $\rightarrow$ Con: have to generate the connected correlation functions for all desired t_{sep}.

Example (TFF η, η')

- Plot integrand $\tilde{A}(\tau)$ for every τ as a function of t_{sep}.
- Determine where plateau starts and choose that value of t_{sep} for all $|\vec{q}_1|$

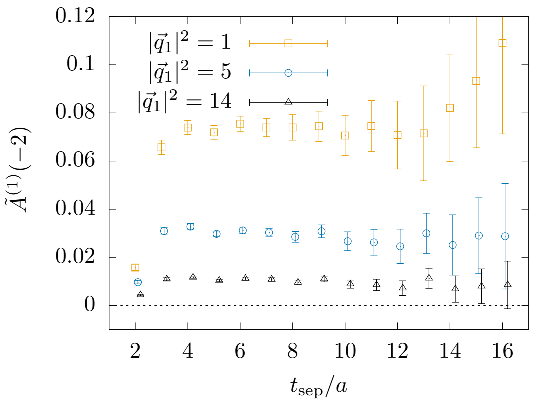

- Plateau behavior between different $|\vec{q}_1|^2$ very correlated.
- Here we would for example choose $t_{sep}/a = 8$ as the start of the plateau.
- We refer to this choice as t_{opt}.
  $\rightarrow$ varying this choice will be part of the systematic

Analysis (TFF η, η')

- Largest noise in the TFF comes from the positive τ part of the integrand.

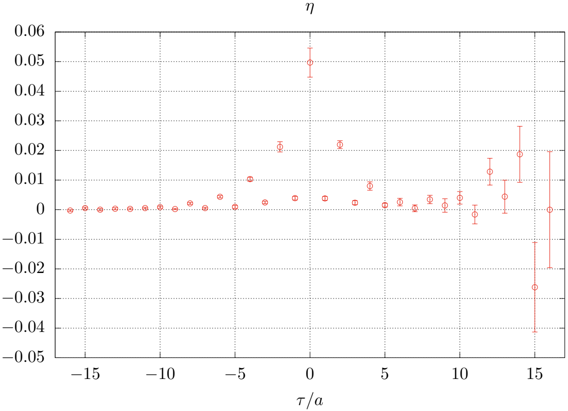

- Integrand between positive and negative τ are related through a Bose symmetry

$$\tilde{A}_{\mu\nu}(\tau, \vec{q}_1, \vec{q}_2) = \tilde{A}_{\nu\mu}(-\tau, \vec{q}_2, \vec{q}_1) e^{-E_p \tau} \tag{1}$$

- Use this relation to take weighted average over postive and negative τ.

Test Assumptions

- Two central assumptions have been made
  1. Choice of t_{opt}.
  2. Weighted average over positive & negative τ using Bose symmetry.

  $\rightarrow$ assumptions can be tested for the π^0 TFF (more precise data)
- Look at the effect of individual assumptions and their combination

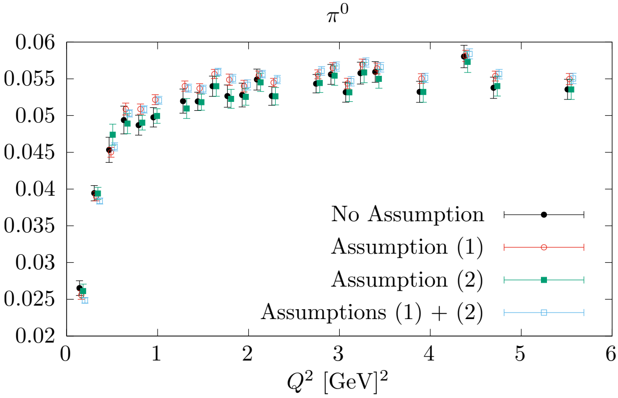

- Effect of assumption (2.) is very small, while (1.) is visible but still mostly within 1σ

Consistency Check

- Relevant consistency check: use the choice of t_{opt} and to check whether adding or subtracting units of time Δt_{opt} significantly changes the result of a_μ.

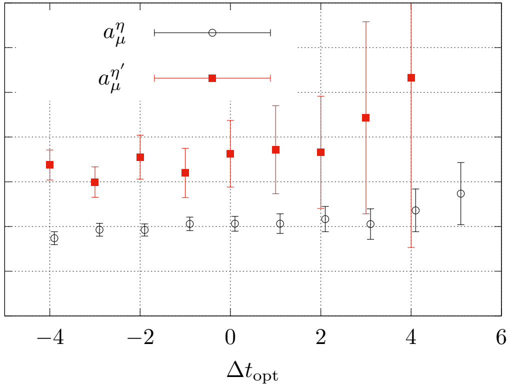

- For $L/a = 32$ $a = 0.0952$ fm (3fm box).
- We see that the signal is really stable for η, η' when adding units of time.
- Below t_{opt} some (staggered) oscillations are present and the stability is slightly less clear.

η Transition Form Factor Integrand

- PVV and P-VV together form the bulk of the signal.
- PV-V and P-V-V contributions are significantly smaller.

$\rightarrow$ When computing the TFF we currently ignore the PV-V and P-V-V.

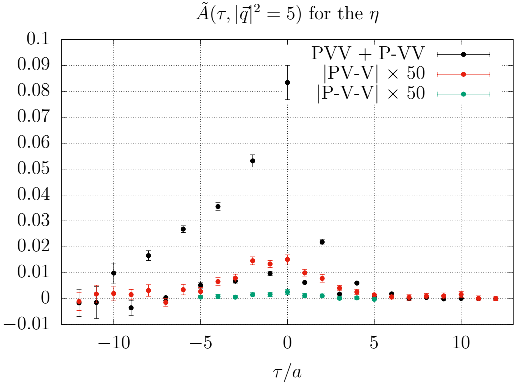

- Ensemble with $L/a = 32$, $a = 0.1315$ fm (4fm box).

η' Transition Form Factor Integrand

- PVV and P-VV together form the bulk of the signal.
- PV-V and P-V-V contributions are significantly smaller.

$\rightarrow$ When computing the TFF we currently ignore the PV-V and P-V-V.

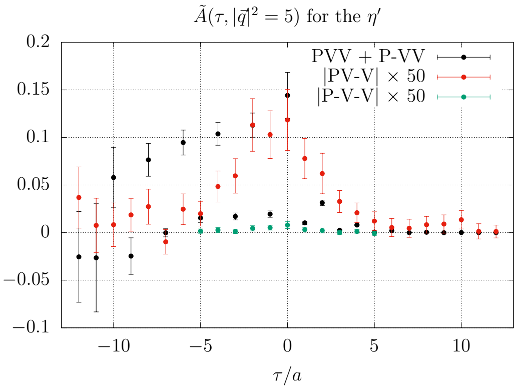

- Ensemble with $L/a = 32$, $a = 0.1315$ fm (4fm box).

η, η' TFF: Result on a Single Ensemble

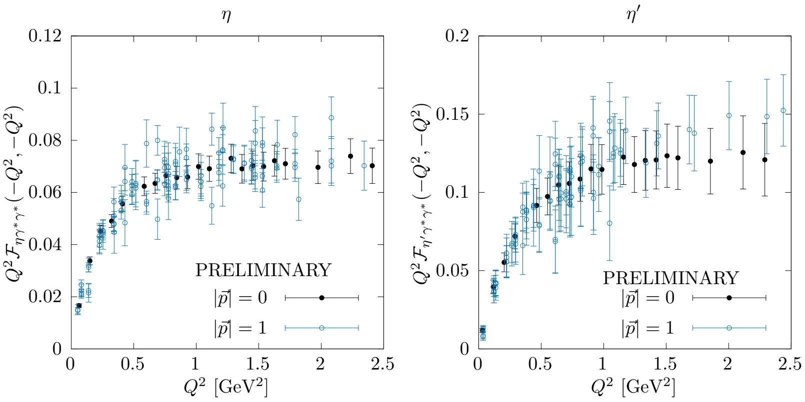

- Ensemble with $L/a = 32$, $a = 0.1315$ fm.
- Good agreement between the two $\eta^{(\prime)}(\vec{p})$ frames with $\vec{p} = \vec{0}$ & $\vec{p} = \frac{2\pi}{L}(0,0,1)$.
- Errors larger than for π^0 because of difficulties mentioned before.
- Statistical error only.

η, η' TFF: Result on a Single Ensemble

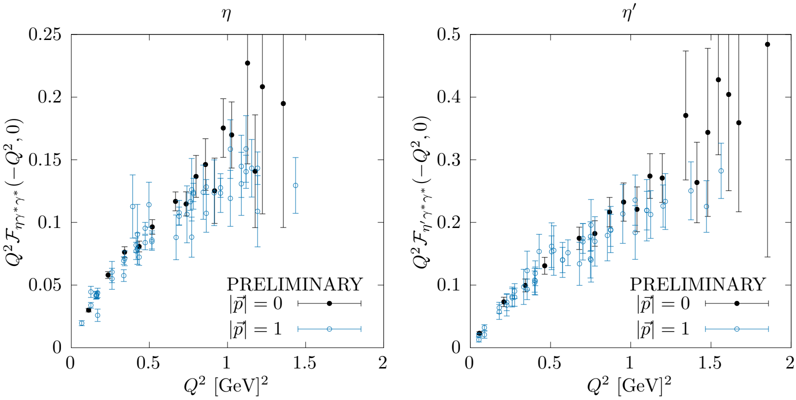

- Ensemble with $L/a = 32$, $a = 0.1315$ fm.
- Good agreement between $\vec{p} = \vec{0}$ & $\vec{p} = \frac{2\pi}{L}(0,0,1)$.
- Preliminary z-expansion fits with N=2 at this lattice spacing give

$$a_\mu^{\eta\text{-pole}}\Big|_{a=0.1315\text{fm}} = 28[5] \times 10^{-11},$$
$$a_\mu^{\eta'\text{-pole}}\Big|_{a=0.1315\text{fm}} = 30[10] \times 10^{-11} \qquad \text{(stat error only)}.$$

Summary

1. Spectrocopy η, η' mesons
   - We now have data on 23 ensembles.
   - Gauge noise reached for 1-point correlators.
   - Final analysis ongoing.
2. Transition Form Factors η, η'
   - TFF at finite lattice spacing looks promising.
   - Data on several lattice spacings has already been generated.
3. Outlook
   - TFF: Add at least one large volume (6fm box) $\rightarrow$ better resolution in Q^2.
   - Deal with the systematics of both projects by variations in the analyses.
   - Do the relevant continuum extrapolations.

References

Altmeyer, R., Born, K. D., Gockeler, M., Horsley, R., Laermann, E., and Schierholz, G. (1993). The Hadron spectrum in QCD with dynamical staggered fermions. *Nucl. Phys. B*, 389:445–512.

Aoki, S., Fukaya, H., Hashimoto, S., and Onogi, T. (2007). Finite volume QCD at fixed topological charge. *Physical Review D*, 76(5).

Aoyama, T. et al. (2020). The anomalous magnetic moment of the muon in the Standard Model. *Phys. Rept.*, 887:1–166.

Borsanyi, S. et al. (2021). Leading hadronic contribution to the muon magnetic moment from lattice QCD. *Nature*, 593(7857):51–55.

Burri, S. A. et al. (2022). Pion-pole contribution to HLbL from twisted mass lattice QCD at the physical point. *PoS*, LATTICE2021:519.

Gérardin, A., Meyer, H. B., and Nyffeler, A. (2016). Lattice calculation of the pion transition form factor $\pi^0 \to \gamma^* \gamma^*$. *Phys. Rev. D*, 94(7):074507.

Gérardin, A., Meyer, H. B., and Nyffeler, A. (2019). Lattice calculation of the pion transition form factor with $N_f = 2+1$ Wilson quarks. *Phys. Rev. D*, 100(3):034520.

Golterman, M. F. L. (1986). STAGGERED MESONS. *Nucl. Phys. B*, 273:663–676.

References

Hoferichter, M., Hoid, B.-L., Kubis, B., Leupold, S., and Schneider, S. P. (2018). Dispersion relation for hadronic light-by-light scattering: pion pole. *Journal of High Energy Physics*, 2018(10).

Ji, X. and Jung, C. (2001). Studying hadronic structure of the photon in lattice QCD. *Physical Review Letters*, 86(2):208–211.

Knecht, M. and Nyffeler, A. (2002). Hadronic light-by-light corrections to the muon $g-2$: The pion-pole contribution. *Physical Review D*, 65(7).

Larin, I. et al. (2020). Precision measurement of the neutral pion lifetime. *Science*, 368(6490):506–509.

Michael, C., Ottnad, K., and Urbach, C. (2013). η and η' masses and decay constants from lattice qcd with 2+1+1 quark flavours.

Neff, H., Eicker, N., Lippert, T., Negele, J. W., and Schilling, K. (2001). Low fermionic eigenmode dominance in qcd on the lattice. *Physical Review D*, 64(11).

Ottnad, K. and Urbach, C. (2018). Flavor-singlet meson decay constants from $N_f = 2+1+1$ twisted mass lattice QCD. *Phys. Rev. D*, 97(5):054508.

PDG (2020). Review of Particle Physics. *PTEP*, 2020(8):083C01.